

Influence of the design of fresh-cut food washing tanks on the growth kinetics of Pseudomonas fluorescens biofilms

Laurent Bouvier, Charles Cunault, Christine Faille, Heni Dallagi, Laurent Wauquier, Thierry Bénézech

▶ **To cite this version:**

Laurent Bouvier, Charles Cunault, Christine Faille, Heni Dallagi, Laurent Wauquier, et al.. Influence of the design of fresh-cut food washing tanks on the growth kinetics of Pseudomonas fluorescens biofilms. iScience, 2021, 24 (6), pp.102506. 10.1016/j.isci.2021.102506 . hal-03247991

HAL Id: hal-03247991
https://hal.inrae.fr/hal-03247991

Submitted on 3 Jun 2021

HAL is a multi-disciplinary open access archive for the deposit and dissemination of scientific research documents, whether they are published or not. The documents may come from teaching and research institutions in France or abroad, or from public or private research centers.

L'archive ouverte pluridisciplinaire **HAL**, est destinée au dépôt et à la diffusion de documents scientifiques de niveau recherche, publiés ou non, émanant des établissements d'enseignement et de recherche français ou étrangers, des laboratoires publics ou privés.



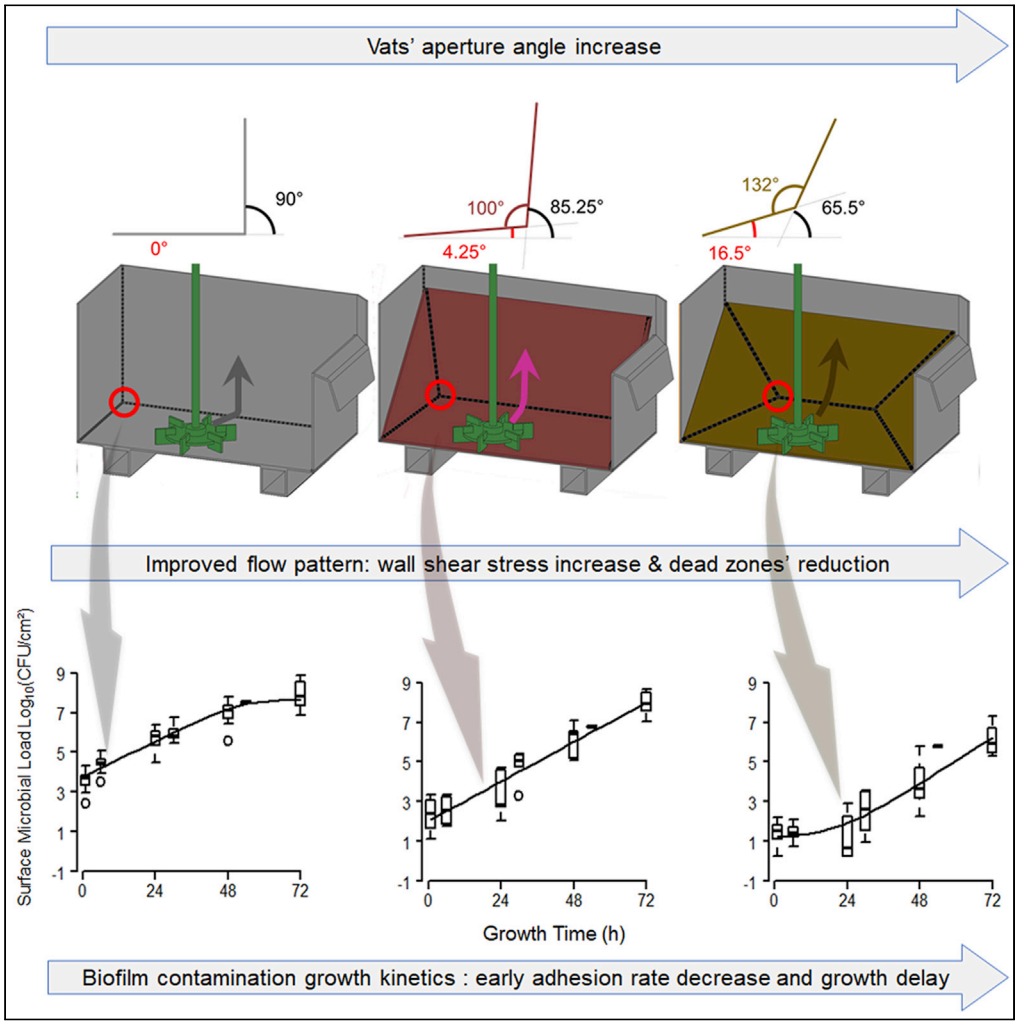
Distributed under a Creative Commons Attribution - NonCommercial - NoDerivatives 4.0 International License

iScience

CellPress
OPEN ACCESS

Article

Influence of the design of fresh-cut food washing tanks on the growth kinetics of *Pseudomonas fluorescens* biofilms



Laurent Bouvier, Charles Cunault, Christine Faille, Heni Dallagi, Laurent Wauquier, Thierry Bénézech

thierry.benezech@inrae.fr

Highlights

Pseudomonas fluorescens biofilm growth kinetics strongly related to the vat design

Improved design lead to 24hr lag time before the biofilm exponential growth phase

Corners, welds, and wetting front areas contamination could be largely mitigated

Bouvier et al., iScience 24, 102506
June 25, 2021 © 2021 The Authors.
https://doi.org/10.1016/j.isci.2021.102506

iScience

CellPress
OPEN ACCESS

Article

Influence of the design of fresh-cut food washing tanks on the growth kinetics of *Pseudomonas fluorescens* biofilms

Laurent Bouvier,[1] Charles Cunault,[2] Christine Faille,[1] Heni Dallagi,[1] Laurent Wauquier,[1] and Thierry Bénézech[1,3,*]

SUMMARY

Mitigation of cross-contamination of fresh-cut food products at the washing step was studied by investigating how the vat design would affect the biofilm contamination surfaces. Hygienic design features such as no horizontal surfaces and only open angles exceeding 100° were proposed. The flow organization (velocity streamlines, wall shear stresses, and dynamics of the flow) was identified by means of computational fluid dynamics (CFD) calculation. *Pseudomonas fluorescens* PF1 biofilm growth kinetics were then mapped. The change in some geometrical features induced a better flow organization reducing "dead zones". This significantly changed the biofilm growth kinetics, delaying the detection of biofilms from 20 hr to 24 hr. Critical areas such as welds, corners, and interfaces appeared far less prone to strong bacterial development. This would mean milder or less chemicals required at the washing step and faster and easier cleaning.

INTRODUCTION

In agro-food industrial environments, such as breweries, dairies, poultry or meat processing factories, as well as fresh-cut industries, surfaces have been reported to be contaminated by a range of microorganisms, including pathogenic and spoilage bacteria (Srey et al., 2013). Once introduced, many bacteria are able to persist on the contaminated surfaces, or even to form biofilms if environmental conditions are suitable. This may lead to cross-contamination of food and beverages at all food processing stages. For example, it has been proven that an outbreak of *Listeria monocytogenes* in Washington State (USA) was due to the contamination of a milkshake machine (Kase et al., 2017). Indeed, the ability of *L. monocytogenes* to survive cold temperatures or desiccation, together with its capability to form biofilms or to integrate pre-existing biofilms, improves its chances of colonizing and persisting in food processing environments (Pang et al., 2019). This phenomenon has been demonstrated in both dairy (Melero et al., 2019) and ready-to-eat food processing facilities (Henriques et al., 2014). Among the numerous abiotic parameters affecting biofilm formation, equipment design and material surface properties comprising topography and physico-chemistry, would play major roles (Faille et al., 2018). Indeed, biofilms are often found in specific areas including those with surface irregularities (e.g., weld features, groves, and scratches) and those affecting flow patterns (e.g., obstacles, dead ends). When biofilms are formed under dynamic conditions, their 3D structures are deeply affected by the flow pattern (Cunault et al., 2015, 2019; Manz et al., 2005;Simões et al., 2006). More compact and less porous biofilms have been observed under turbulent flows than under laminar flow conditions (Stoodley et al., 1999a; Vieira et al., 1993). In recent work (Cunault et al., 2018, 2019), surface contamination by *Pseudomonas fluorescens* PF1 biofilms has been studied using pilot scale washing tanks with the standard design features encountered in the fresh-cut vegetable processing industry. It has been found that biofilm growth dynamics (Cunault et al., 2018) and structures (Cunault et al., 2019) depend on the location in the tanks, which could range from discontinuous monolayer biofilms to biofilms with large, thick clusters. Poor design features encountered in such tanks make surface contamination difficult to remove. These include horizontal surfaces, right angles, and sometimes, poor quality welds and the presence of closed corners at the vat bottom and are critical in terms of hygiene.

Many efforts have been made to control biofilm development by preventive and curative approaches (Amin et al., 2020; Muhammad et al., 2020; Rajab et al., 2018; Srey et al., 2013; Whitehead et al., 2015). Among the preventive approaches, several strategies have been developed in attempts to prevent biofilm installation,

[1]Univ. Lille, CNRS, INRAE, Centrale Lille, UMR 8207 - UMET - Unité Matériaux et Transformations, F-59000 Lille, France

[2]IATE, Univ Montpellier, INRAE, Institut Agro, Montpellier, France

[3]Lead contact

*Correspondence: thierry.benezech@inrae.fr

https://doi.org/10.1016/j.isci.2021.102506

This is an open access article under the CC BY-NC-ND license (http://creativecommons.org/licenses/by-nc-nd/4.0/).

primarily by acting on surface material properties or equipment design (Faille et al., 2018). Today, hygienic food equipment design is now fully recognized as a key to mitigate surface contamination and biofilm installation, as well as allowing efficient cleaning (Faille et al., 2018). Numerical fluid mechanics approaches assist in improving cleanability when designing food equipment or installing accessories (Asteriadou et al., 2006; Blel et al., 2009; Cunault et al., 2015; Kawale and Chandramohan, 2017). Such tools allow the evaluation of some relevant parameters, such as the local mean shear stress which impacts both soiling (Cunault et al., 2015) and cleaning (Kawale and Chandramohan, 2017). Unfortunately, computational fluid dynamics (CFD) methods do prove to be time-consuming (Blel et al., 2009).

Consequently, the aim of this study was to investigate how the application of some hygienic design guidelines (www.ehedg.org), regarding open angles and corners, wall inclination or the suppression of horizontal surfaces, could radically change the dynamics of biofilm growth on equipment surface. For this purpose, a series of mock-ups of industrial washing tanks for the fresh-cut food industry as recently proposed by (Cunault et al., 2018) was used to study the contamination patterns of *P. fluorescens* PF1 biofilms. Such biofilms might also support the growth of pathogenic bacteria such as *L. monocytogenes* on inert surfaces found in food processing equipment (Carpentier and Chassaing, 2004).

RESULTS

CFD analysis of the flow organization in the vats

The velocity streamlines are presented for both orthogonal and modified geometries in Figure 1.

The flow is clearly homogeneous in the alternative geometry as demonstrated by the disappearance of the large recirculation zones observed at the four corners of the vat with an orthogonal configuration.

This was confirmed by comparing the Videos S1 and S2 (supplemental information) visualizing the flow dynamics created by a complete impeller rotation. The Video S1 described the velocity vector variation of a slice perpendicular to the inlet flow, showing the appearance of small recirculation zone on the left (132° internal angle) and which disappeared on the right (100° angle). However, such recirculation phenomenon appeared minor when compared to the significant down-pumping and recirculation area in the orthogonal configuration described in (Cunault et al., 2015) (Video S2). The modified geometry appeared to drastically reduce what can be called 'dead zones'.

At each swabbed area of both vat geometries the minimum and the maximum average WSS (WSSavmin and WSSavmax) were calculated over a complete impeller rotation. The data obtained are presented in Figure 2.

On comparing the three different apertures, it is clear that the alternative geometry presents more homogeneous WSS values. However, all corners, whatever the vat, appeared to present the lowest WSS values. In addition, the proximity to the impeller imposed the largest WSS variations. Indeed, the WSS reached 4 Pa for the average minima and 5 Pa for the average maxima compared to general variations for the other zones only ranging from 0.001 to 1 Pa. Nevertheless, these high shear stress values of 4 and 5 Pa were only observed in the orthogonal vat, as maxima reached in modified geometry vats were only 1.19 and 1.31 Pa for the average minimum and the average maximum respectively. The dynamics of the WSS fluctuations for all areas were visualized by the Videos S1 and S2. These show that the WSS fluctuations imposed by the Rushton impeller decreases rapidly the farther the measurement from the impeller in both geometries.

Biofilm growth curves

The surface microbial load (SML) were represented with a box plot over time for all trials together, according to sample location. Curve fittings from the Baranyi model were also plotted, considering all the data obtained. The results in Figures 3 and 4 respectively presented growth curves on either corners and welds or on vat walls.

Comparing 90° apertures to 100° and 132°, strong differences in growth curve shapes can be seen. In fact, at 90° aperture, the growth curves reached a plateau value at 48 hr of growth for corners and horizontal welds. Such a plateau exists neither for corners nor for horizontal welds at 100° and 132° apertures or for any other areas tested. More interestingly, for both 100° and 132°apertures, the biofilm growth only started visibly after 24 hr corresponding to a lag phase except for corners (100° aperture) and for inclined welds 4°

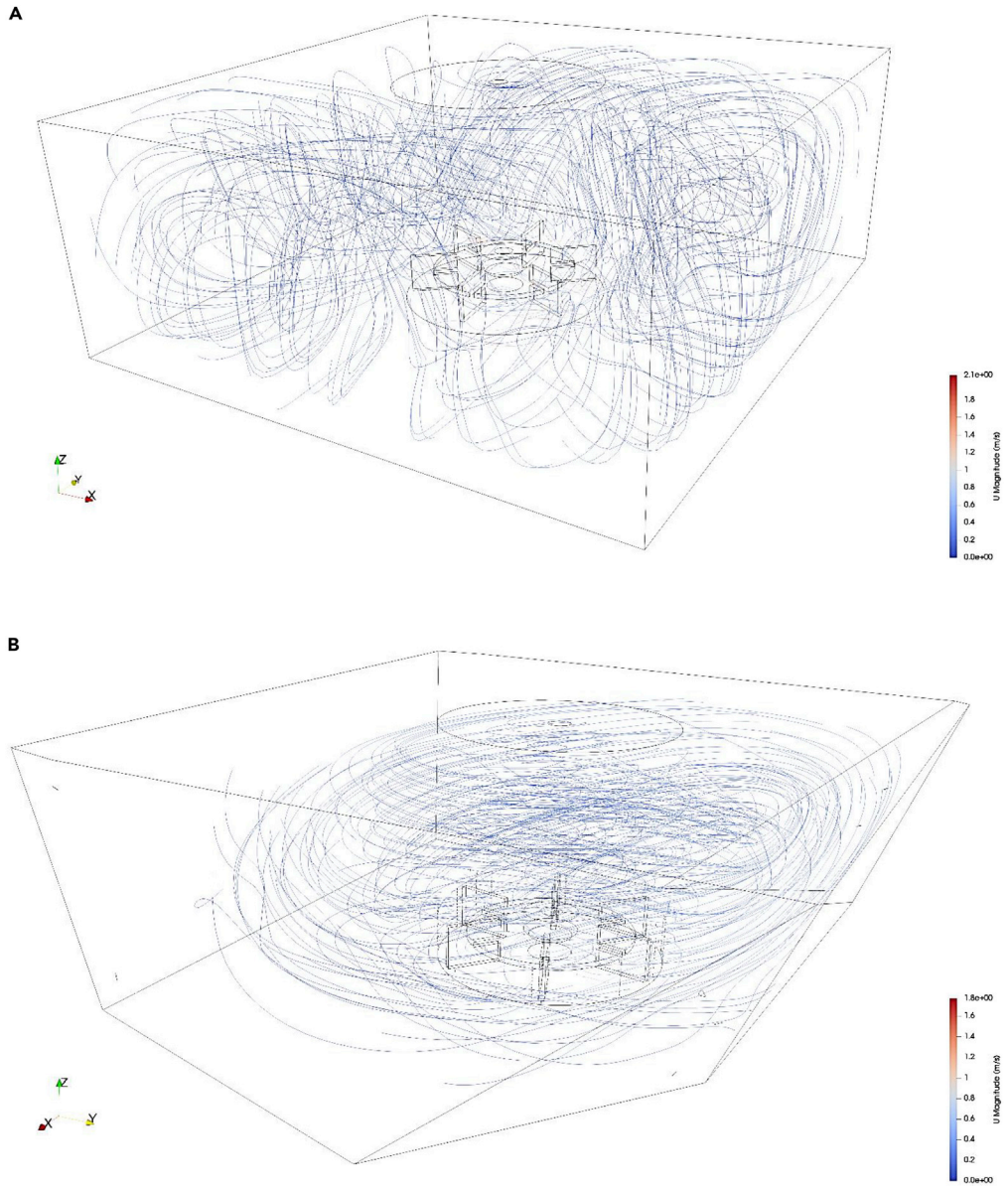


Figure 1. Velocity streamlines generated by the impeller for the two vats

(A) cubic – commonly encountered features;

(B) improved geometry.

and 16° not directly affected by the flow induced by the proximity of the impeller. Such remote welding zones, whatever the aperture, were prone to a quick contamination of between 1 and 2 Log_{10} cm^{-2}, as was observed for the other areas, but this was then followed by an exponential growth phase. It is thus surprising to notice such a marked difference in the growth curves on 85° and 65° inclined welds, which presented lag phases respectively of around 24 hr and 30 hr. The flat surfaces (Figure 4) could be presented in three groups, the bottom walls, the border walls, and the air/liquid/wall interfaces areas. In all cases with the 100° and 132° apertures, the biofilm growth started after at least a 24-hr apparent lag phase in contrast to those of 90° aperture. Interface areas were also affected by this phenomenon, with an apparent lag phase of 24 hr for both 100° and 132° apertures.

Box plots of the variation of the three parameters λ, μ_{max} and N_0 against the aperture, the different features and the angles were presented in Figure 5.

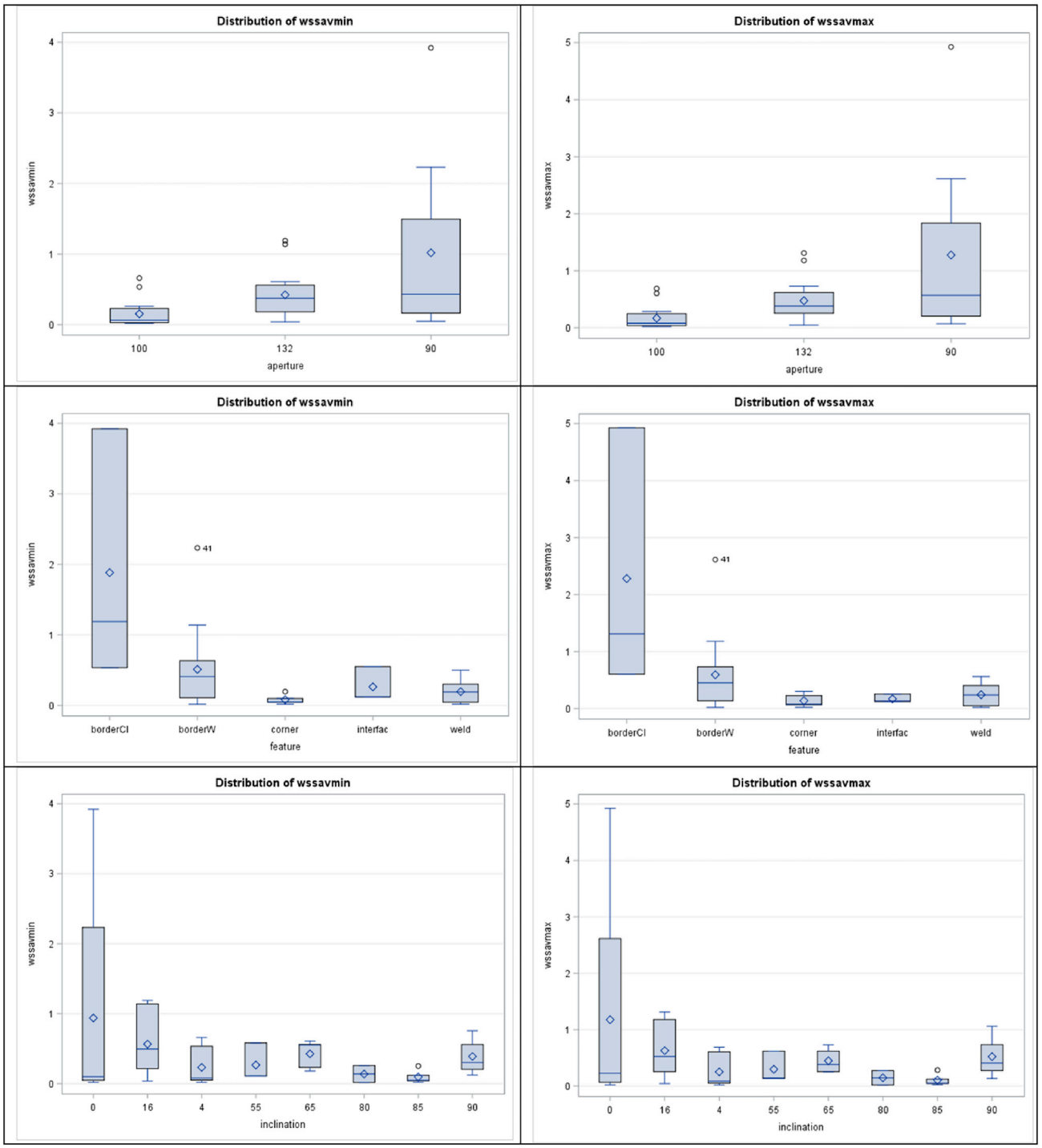


Figure 2. Box plots displaying the distribution of the average minimum and of the average maximum values of the WSS calculated over a complete rotation of the impeller per selected swabbing areas against (1) the aperture (90°, 100° and 132°); (2) the surface feature: border CI (side wall close to the impeller), border W (side wall), corner, interface, and weld; or (3) the inclination for the different zones.

The observed wide variability in the λ data appeared to be explained by the role of the other selected explanatory variables, such as the aperture, the surface feature, and the wall inclination according to the Kruskal-Wallis rank sums tests followed by a Pairwise two-sided multiple comparison analysis. When considering only the apertures, a significant difference was observed between the alternative vat

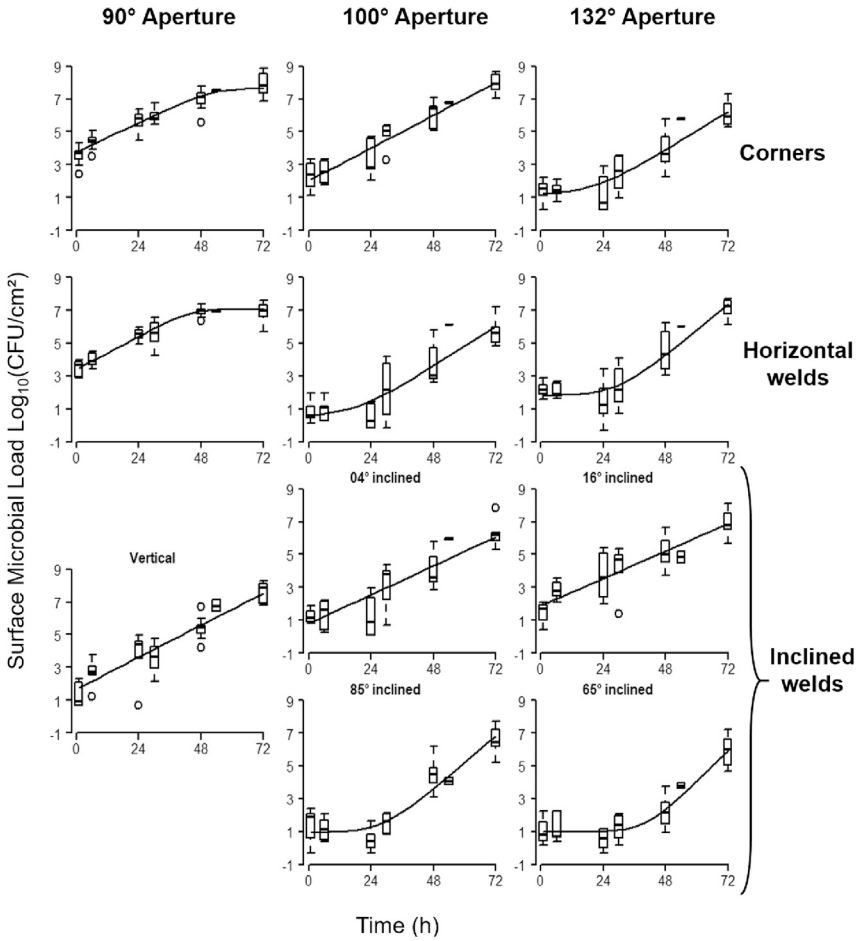


Figure 3. Growth curves observed for corners and welds

geometries (100° and 132°) and the orthogonal one where the median value of λ being null. In addition, significant differences were observed between inclinations of 55°, 65°, 80° (the largest λ with a median value of over 30 hr) or 85° and those of the orthogonal vat (0° and 90°). The two slighter inclinations 4° and 16° (bottom part, modified vat geometries whatever the proximity to the impeller) appeared to be different from the inclination 65°. λ values also varied greatly with some geometry features when comparing vat border walls, bottom walls, corners, and welds. On biofilms grown on the vat border walls, λ was found to be significantly higher than for corners and welds, although not in the bottom areas.

An opposing trend was observed to a lesser extent for the maximum growth rate μ_{max}, observed in modified geometries and allowing higher growth rates. In addition, the μ_{max} was found to be significantly lower on corners and border walls, as they are apparently prone to the greatest biofilm growth after the lag phase.

The modeledN_0 did not depend on its position in relation to the impeller. However, an aperture of 90° led to significantly higher initial contamination than the 100° and 132°apertures tested. In addition, corners and welds presented significantly higher initial contaminations. Only the inclination of 0° (horizontal surfaces, orthogonal vats) was found to be significantly different from the other inclinations with a N_0 over 2 $\log_{10}$ cm^{-2} (median value).

DISCUSSION

CFD has been used with greater and greater success for the study of flow in complex systems, thanks to validation through experimentation. In addition, flow induced by a Rushton impeller has been extensively

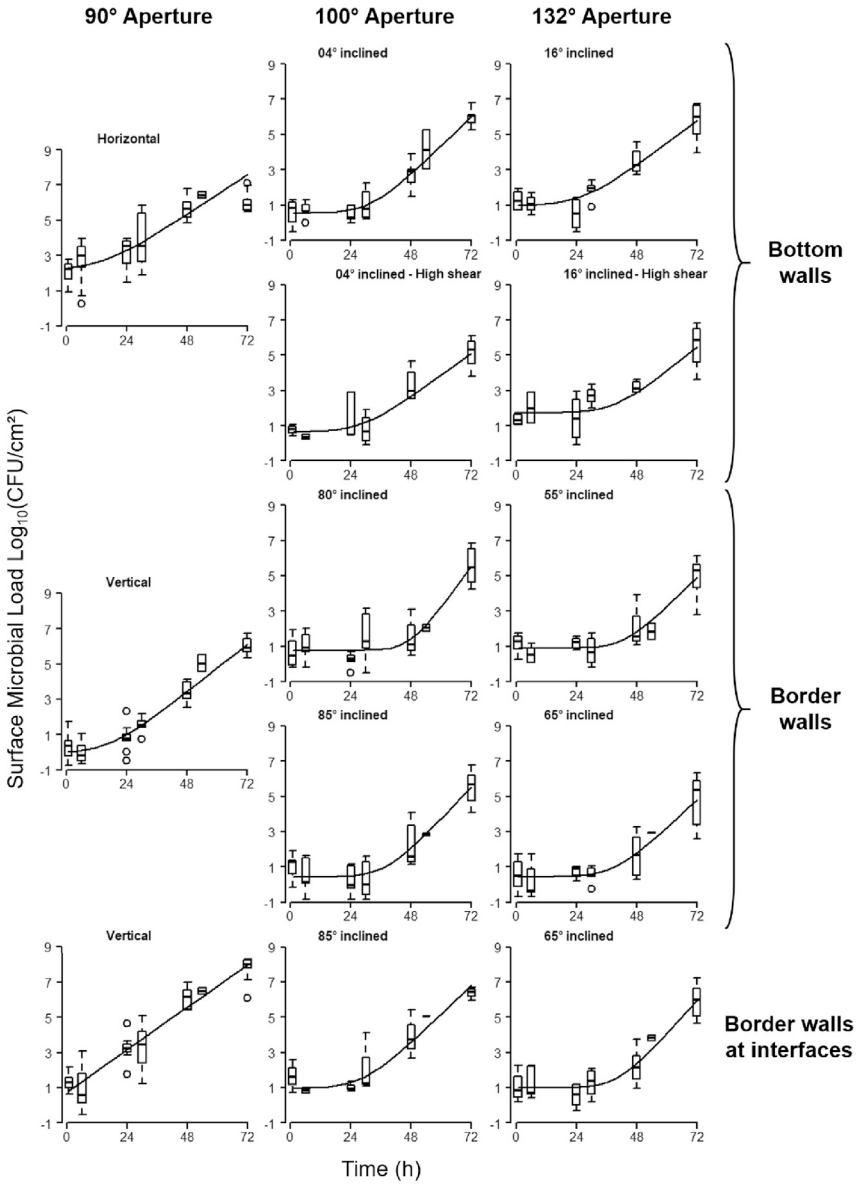


Figure 4. Growth curves obtained for all flat surfaces

studied in the literature and CFD approaches are now common (Torotwa and Ji, 2018). Previous work allowed us to validate the CFD modeling through experimentation on the orthogonal vat (Cunault et al., 2015) and this approach was developed here to describe the changes in both the flow organization and wall shear stress repartition induced by modified geometry. Significant flow changes were observed, including better mixing in the modified tank and a quite homogeneous WSS repartition, corners excepted. However, such geometrical features of the orthogonal vat can be automatically ruled out in terms of design according to EHEDG guidelines (available at www.ehedg.org). In current fresh-cut food industries washing tanks, although no impeller is used, flow organization homogeneity could be sought, as this limits the possibility of recirculation areas which are again considered to be a design-induced hygienic shortcoming. Previous works have highlighted the importance of preventing such recirculation zones to avoid both the trapping of the contamination and to improve cleaning efficiency (Blel et al, 2009, 2010, 2013).

The contamination scheme in the alternative vat geometries were compared to previous experiments (Cunault et al., 2015, 2018) carried out on vats designed to be close to those encountered in the fresh-cut food

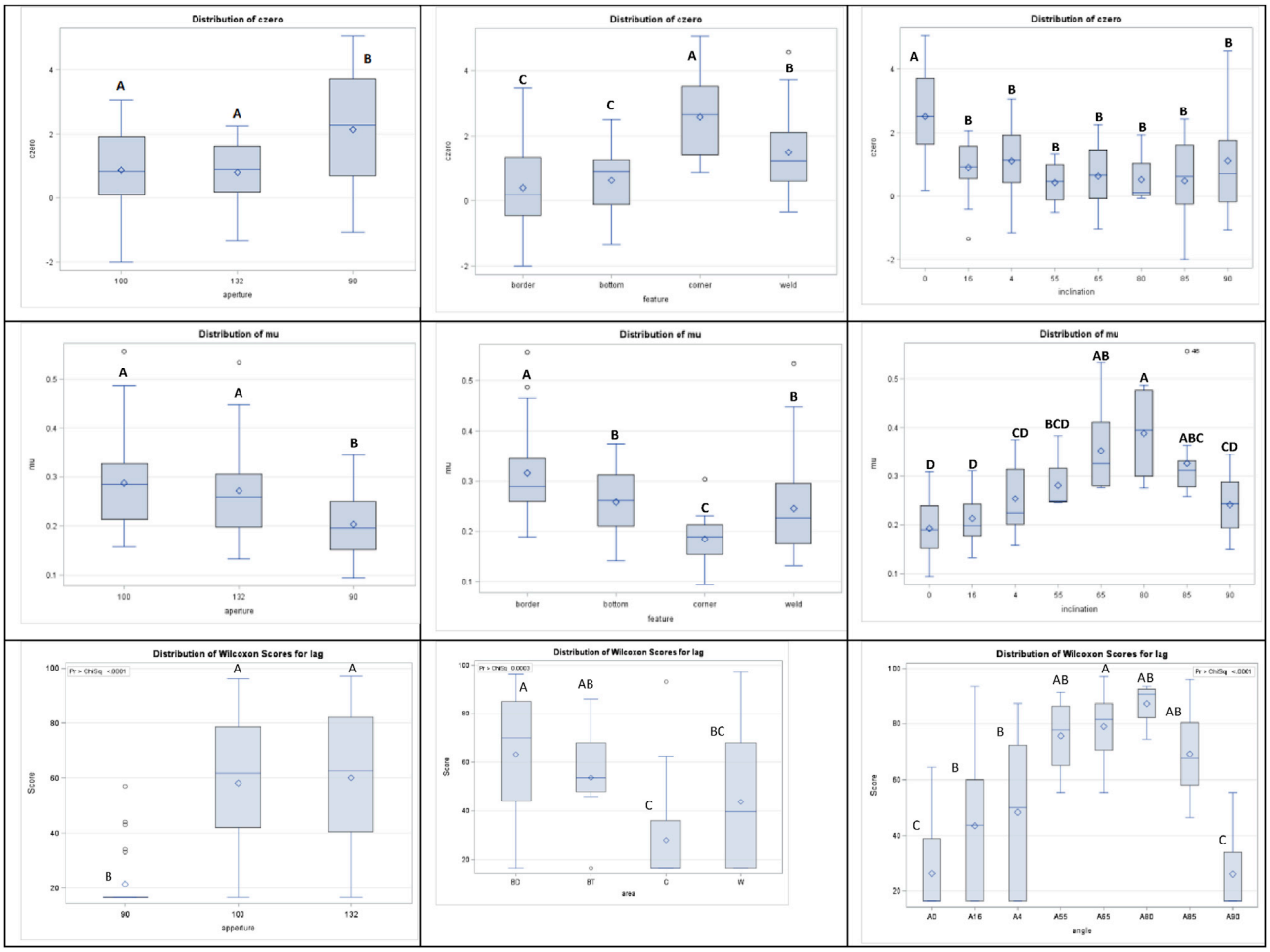


Figure 5. Boxplots of the distribution of the kinetics parameters according to (1) the aperture 90°, 100° and 102°, (2) the following features, border (BD) or bottom walls (BT), corners (C) and weld (W) and (3) the inclination from 0° up to 85°. The ANOVA procedure (boxplots) and Tukey's Studentized Range (HSD) Test was applied for the initial surface contamination (czero) and the maximum growth rate (mu). The Kruskal-Wallis rank sums tests were followed by a Pairwise two-sided multiple comparison analysis for the apparent lag phase (lag) presented with the distribution of Wilcoxon scores. Common letters meaning no significant differences.

industry. The alternative geometries were chosen as they comply with EHEDG principles (EHEDG Document number 8, 2018 third edition), having open angles, no horizontal surfaces thereby inducing good drainage and no recirculation areas.

Biofilm growth kinetics were mapped inside the vat modified surfaces and compared to those mapped in the orthogonal ones. An increase from 10^6 up to 5 10^7CFU/mL was observed after 72 hr in the circulating liquid as detailed previously (Cunault et al., 2018) for the orthogonal vat. The huge differences observed within the SML growth kinetics of the areas tested whatever the vat geometry could not be explained by this increase of the circulating contamination. In consequence, the vat design clearly impact the SML and the biofilm development. The literature reports numerous studies on how the flow conditions affect biofilm formation. Some authors mainly working with flow cells (Chmielewski and Frank, 2003; Dunsmore et al., 2002; Hödl et al., 2014; Purevdorj et al., 2002; Stoodley et al., 1999b) have shown that adequate flow design reduces biofilm development as migrating cells and cluster spatial coalescence are inhibited.

The major effect observed in this study was the presence of a lag phase, which affected most areas except for the welds. Even corners with an opening of 132° showed a lag phase that lasted for at least 10 hr. This time period is sufficient for a standard production time in a fresh-cut food factory.

This phenomenon was discussed previously (Cunault et al., 2018) as it is observed at a much lower extent on the orthogonal vat. The lag period occurred after a short period of initial adhesion of the planktonic form (their physiological state being that of the exponential phase). Thus, the biofilm lag periods could not be related to any lag phase of the former planktonic cells. When no lag phase, this initial adhesion could be significant (from 10^2 up to 10^3CFU/cm^2) on most of the areas of the orthogonal vats followed by an exponential increase in the biofilm load as observed on the kinetics growth curves.

A quantitative estimate of *P. fluorescens* AR 11 biofilms development (Recupido et al., 2020) was carried out under three different flow conditions (stagnant, shaken fluid, or controlled laminar conditions) for 72 hr. Under stagnant conditions, 24 hr was sufficient to reach a plateau after a rapid increase during the first 5 hr. Under shaken conditions, the main difference was a higher biomass amount obtained than for static conditions. Conversely, under flow cell conditions, an erosion-induced lag phase was observed lasting at least 24 hr which can be considered in line with our work observations.

Another recent study (Bucs et al., 2018) stated that the biofilm control strategies in spiral-wound membranes should focus on delaying the biofilm formation, thereby permitting more efficient removal by further cleaning strategies. This delay in the biofilm development depended in that case, as in our work, largely on the flow conditions. It was shown (Moreira et al., 2013) a reduced *Escherichia coli* biofilm formation under higher shear stress conditions because the adverse effects of the shear stress were more significant than the improvement of nutrient mass transfer. Here this is more the dynamics induced by the flow than the absolute value of the shear stress which plays a role on the presence of an apparent lag phase. A similar trend was observed previously on the impact of the flow organization on bacteria removal in closed systems (Blel et al., 2010, 2013).

In this study, the growth rate was clearly reduced in corners, despite a significantly higher initial adhesion and almost no lag phase. For the other areas, the higher growth rate observed was probably induced by better mixing in the near wall region being favorable for the biofilm development. When comparing high shear with low shear zones, apparently no difference in the growth rate could be observed, with the high shear areas likely to be prone to biofilm erosion phenomenon.

Hydrodynamics are known to affect cell density and biofilm matrix composition. The fluid velocity field in contact with the attached microbial layer is widely considered as one of the most important factors affecting not only the biofilm's structure but also its activity (Araújo et al., 2016; Liu and Tay, 2002; Pereira et al., 2002). This greatly exceeds the influence of factors, such as biofilm age, suspended cell concentration, pH, and surface roughness of the substratum (Chen et al., 2005). Indeed, biofilm volumetric density and EPS volume increase with the shear stress, resulting in increased biofilm cohesion (Garny et al., 2008; Simões et al., 2010). Such statements were confirmed with a stronger resistance to shear (Cunault et al., 2019) observed for biofilms grown on the vertical walls of the orthogonal vat compared, e.g., to corners.

Specificity for the biofilms grown at the interface air/material/water (ALW) (Cunault et al., 2019) was observed in terms of structure and resistance to the mechanical or chemical actions. The observed higher resistance was the result of the conditions encountered during biofilm formation at the air-liquid-substratum interface, along with the periodic wetting induced by the impeller rotation. Indeed, it is largely observed that thick biofilms often preferentially develop at the air-liquid-substratum interface, rather than in wholly submerged areas. Recently, the same *P. fluorescens* strain (Jha et al., 2020) was used and compared to three other strains *E. coli*, *Bacillus cereus*, and *Bacillus subtilis* to form biofilms in static conditions at the ALW interface on four materials with very different topographic and hydrophilic/hydrophobic properties (stainless steels with 2R or 2B finishes, polypropylene and glass). After one day of incubation in a bacterial suspension, all but *B. cereus* was found to form large amounts of biofilm, easily observable to the naked eye with a 3D structure at the interface corresponding to the meniscus area. After a standard cleaning-in-place treatment involving NaOH 0.5% at 60°C, cultivable cells were only detected from *B. cereus* biofilms (growth on agar), while biofilms were also still visible on coupons contaminated with *P. fluorescens*. Furthermore, most residual biofilms on the coupons after cleaning appeared orange by epifluorescence microscopy after staining with orange acridine suggesting the presence of many viable but non-culturable cells within the residual biofilms. All these results highlighted the importance of biofilms at the ALW interfaces in the control of surface hygiene, particularly in the food industry.

It is interesting here to note that significant lag phases were observed for these specific areas (>30 hr) with both apertures 100° and 132°. This means that the issue represented by the interface in this particular case could be solved by modifying the geometry.

The improvement in the mitigation of the biofilm development for at least the first 24 hr (apparent lag phase), demonstrated the importance of hygienic design principles (Hofmann et al., 2018) which states that both horizontal surfaces and corners should be avoided. In a previous work (Cunault et al., 2019), resistance to cleaning for weld areas was largely lowered when these were placed vertically (vat with 90°aperture), given that welds could be considered as a minor shortcoming, with the right geometry.

Considering horizontal welds in orthogonal vats, the biofilm growth kinetics reached a plateau after 48 hr and obviously no lag phase was observed. Nevertheless, a marked change was observed for horizontal welds in the presence of 100° and 132° apertures. Indeed, a lag phase of around 20 hr was observed. One can note that inclined welds at 4° and 16° presented no lag phase. These areas thus seemed to be less affected by the flow induced by the impeller not explained by the wall shear stress, which was close or even higher than for most of the other areas. Previous papers have stated that there are no clear relationships between welding zones and bacterial adhesion (Casarin et al., 2014) or bacterial colonization (Tide et al., 1999), but the flow organization as shown here could either improve the initial adhesion (from 3 to 1 $Log_{10}\,cm^{-2}$ in case of horizontal welds) or accelerate the bacterial colonization scheme, through different biofilm growth kinetics including lag phases.

In conclusion, we have previously demonstrated, in conditions close to those encountered in vegetable processing industry, that some specific areas within industrial washing tanks are prone to allowing a strong bacterial contamination and generating a further high resistance to rinsing/cleaning processes. However, the change in some geometrical features (mainly angles) induced a better flow organization, i.e., better homogeneous mixing deeply changed the biofilm growth kinetics and rendered critical areas (welds, corners, and interfaces) far less prone to bacterial development within a reasonable time lapse for potential industrial applications. Modifications to the design of open machineries (e.g., open angles, no horizontal surfaces) would thus significantly change the contamination scheme and eventually improve the ease of cleaning. This would allow industrialists to envisage the use of more environmentally friendly washing steps (reduction in the use of chemicals) and possibly allow milder cleaning procedures complying with new environmental constraints.

Limitations of the study

All the limitations were mentioned in the transparent methods and discussion parts.

Resource availability

Lead contact

Further information and requests for resources and materials should be directed to and will be fulfilled by the lead contact, Thierry Bénézech (thierry.benezech@inrae.fr).

Material availability

The tested items and the bacteria strain are available on request to the lead contact.

Data and code availability

A finite volume CFD simulation of the alternative geometry tank was achieved under an open source software: OpenFOAM 6 (© OpenCFDLtd,2019;ESI Group).

METHODS

All methods can be found in the accompanying transparent methods supplemental file.

SUPPLEMENTAL INFORMATION

Supplemental information can be found online at https://doi.org/10.1016/j.isci.2021.102506.

ACKNOWLEDGMENTS

We thank Jacky Six for his technical assistance and helpful discussions. This work was undertaken under the European Research Project SUSCLEAN (contract number FP7-KBBE-2011-5, project number: 28514) and was supported by the Interreg programme V France-Wallonie-Vlaanderen Veg-I-Tec project.

AUTHOR CONTRIBUTIONS

L.B. conducted the CFD calculations with H.D. and participated in the writing of the paper regarding CFD. C.C. conducted the experiments and biofilm growth modeling and with C.F. participated to the writing of the paper regarding microbiology. L.W. was in charge to the building of the whole experimental set-up and items. T.B. was responsible for the research and wrote the paper with L.B., C.C. and C.F.

DECLARATION OF INTERESTS

The authors declare no competing interests.

Received: October 28, 2020
Revised: February 25, 2021
Accepted: April 29, 2021
Published: June 25, 2021

REFERENCES

Amin, M., Rowley-Neale, S., Shalamanova, L., Lynch, S., Wilson-Nieuwenhuis, J., El Mohtadi, M., Banks, C.E., and Whitehead, K.A. (2020). Molybdenum disulfide surfaces to reduce Staphylococcus aureus and Pseudomonas aeruginosa biofilm formation. ACS Appl. Mater. Inter. *12*, 21057–21069. https://doi.org/10.1021/acsami.0c02278.

Araújo, P.A., Malheiro, J., Machado, I., Mergulhão, F., Melo, L., and Simões, M. (2016). Influence of flow velocity on the characteristics of Pseudomonas fluorescens biofilms. J. Environ. Eng. *142*, 04016031. https://doi.org/10.1061/(ASCE)EE.1943-7870.0001068.

Asteriadou, K., Hasting, A.P.M., Bird, M.R., and Melrose, J. (2006). Computational fluid dynamics for the prediction of temperature profiles and hygienic design in the food industry. Food Bioprod.Process. *84*, 157–163. https://doi.org/10.1205/fbp.04261.

Blel, W., Legentilhomme, P., Bénézech, T., and Fayolle, F. (2013). Cleanabilty study of a scraped surface heat exchanger. Food Bioprod.Process. *91*, 95–102. https://doi.org/10.1016/j.fbp.2012.10.002.

Blel, W., Legentilhomme, P., Le Gentil-Lelièvre, C., Faille, C., Legrand, J., and Bénézech, T. (2010). Cleanability study of complex geometries: interaction between B. cereus spores and the different flow eddies scales. Biochem. Eng. J. *49*, 40–51. https://doi.org/10.1016/j.bej.2009.11.009.

Blel, W., Pierrat, D., Le Gentil, C., Legentilhomme, P., Legrand, J., Hermon, C., Faille, C., and Benezech, T. (2009). Numerical and experimental investigations of the flow structures through a gradual expansion pipe. Trends Food Sci. Technol. *20*, S70–S76. https://doi.org/10.1016/j.tifs.2009.01.043.

Bucs, S.S., Farhat, N., Kruithof, J.C., Picioreanu, C., van Loosdrecht, M.C.M., and Vrouwenvelder, J.S. (2018). Review on strategies for biofouling mitigation in spiral wound membrane systems. Rev. Res. Dev. Desalination *434*, 189–197. https://doi.org/10.1016/j.desal.2018.01.023.

Carpentier, B., and Chassaing, D. (2004). Interactions in biofilms between Listeria monocytogenes and resident microorganisms from food industry premises. Int. J. Food Microbiol. *97*, 111–122. https://doi.org/10.1016/j.ijfoodmicro.2004.03.031.

Casarin, L.S., Brandelli, A., de Oliveira Casarin, F., Soave, P.A., Wanke, C.H., and Tondo, E.C. (2014). Adhesion of salmonella enteritidis and listeria monocytogenes on stainless steel welds. Int. J. Food Microbiol. *191*, 103–108. https://doi.org/10.1016/j.ijfoodmicro.2014.09.003.

Chen, M.J., Zhang, Z., and Bott, T.R. (2005). Effects of operating conditions on the adhesive strength of Pseudomonas fluorescens biofilms in tubes. Colloids Surf. B Biointerfaces *43*, 61–71. https://doi.org/10.1016/j.colsurfb.2005.04.004.

Chmielewski, R.A.N., and Frank, J.F. (2003). Biofilm formation and control in food processing facilities. Compr.Rev. Food Sci. Food Saf. *2*, 22–32. https://doi.org/10.1111/j.1541-4337.2003.tb00012.x.

Cunault, C., Faille, C., Bouvier, L., Föste, H., Augustin, W., Scholl, S., Debreyne, P., and Benezech, T. (2015). A novel set-up and a CFD approach to study the biofilm dynamics as a function of local flow conditions encountered in fresh-cut food processing equipments. Food Bioprod.Process. *93*, 217–223. https://doi.org/10.1016/j.fbp.2014.07.005.

Cunault, C., Faille, C., Briandet, R., Postollec, F., Desriac, N., and Benezech, T. (2018). Pseudomonas sp. biofilm development on fresh-cut food equipment surfaces – a growth curve – fitting approach to building a comprehensive tool for studying surface contamination dynamics. Food Bioprod.Process. *107*, 70–87. https://doi.org/10.1016/j.fbp.2017.11.001.

Cunault, C., Faille, C., Calabozo-Delgado, A., and Benezech, T. (2019). Structure and resistance to mechanical stress and enzymatic cleaning of Pseudomonas fluorescens biofilms formed in fresh-cut ready to eat washing tanks. J. Food Eng. *262*, 154–161. https://doi.org/10.1016/j.jfoodeng.2019.06.006.

Dunsmore, B.C., Jacobsen, A., Hall-Stoodley, L., Bass, C.J., Lappin-Scott, H.M., and Stoodley, P. (2002). The influence of fluid shear on the structure and material properties of sulphate-reducing bacterial biofilms. J. Ind. Microbiol. Biotechnol. *29*, 347–353. https://doi.org/10.1038/sj.jim.7000302.

Faille, C., Cunault, C., Dubois, T., and Bénézech, T. (2018). Hygienic design of food processing lines to mitigate the risk of bacterial food contamination with respect to environmental concerns. Innov.Food Sci. Emerg. Technol. *46*, 65–73. https://doi.org/10.1016/j.ifset.2017.10.002.

Garny, K., Horn, H., and Neu, T.R. (2008). Interaction between biofilm development, structure and detachment in rotating annular reactors. Bioproc.Biosyst. Eng. *31*, 619–629. https://doi.org/10.1007/s00449-008-0212-x.

Henriques, A.R., da Gama, L.T., and Fraqueza, M.J. (2014). Assessing Listeria monocytogenes presence in Portuguese ready-to-eat meat processing industries based on hygienic and safety audit. Food Res. Int. *63*, 81–88. https://doi.org/10.1016/j.foodres.2014.03.035.

Hödl, I., Mari, L., Bertuzzo, E., Suweis, S., Besemer, K., Rinaldo, A., and Battin, T.J. (2014). Biophysical controls on cluster dynamics and architectural differentiation of microbial biofilms in contrasting flow environments. Environ. Microbiol. *16*, 802–812. https://doi.org/10.1111/1462-2920.12205.

Hofmann, J., Åkesson, S., Curiel, G., Woulters, Dr.P., and Timperley, A. (2018). Hygienic design

principles. Eur. Hyg. Eng. Des.Group Guidel. *8*, 1–13.

Jha, P.K., Dallagi, H., Richard, E., Benezech, T., and Faille, C. (2020). Formation and resistance to cleaning of biofilms at air-liquid-wall interface. Influence of bacterial strain and material. Food Control *118*, 107384. https://doi.org/10.1016/j.foodcont.2020.107384.

Kase, J.A., Zhang, G., and Chen, Y. (2017). Recent foodborne outbreaks in the United States linked to atypical vehicles - lessons learned. Curr.Opin.Food Sci. 56–63. https://doi.org/10.1016/j.cofs.2017.10.014.

Kawale, S., and Chandramohan, V.P. (2017). CFD simulation of estimating critical shear stress for cleaning flat soiled surface. Sādhanā *42*, 2137–2145. https://doi.org/10.1007/s12046-017-0748-z.

Liu, Y., and Tay, J.H. (2002). The essential role of hydrodynamic shear force in the formation of biofilm and granular sludge. Water Res. *36*, 1653–1665. https://doi.org/10.1016/S0043-1354(01)00379-7.

Manz, B., Volke, F., Goll, D., and Horn, H. (2005). Investigation of biofilm structure, flow patterns and detachment with magnetic resonance imaging. Water Sci. Technol. *52*, 1–6.

Melero, B., Stessl, B., Manso, B., Wagner, M., Esteban-Carbonero, O.J., Hernandez, M., Rovira, J., and Rodriguez-Lazaro, D. (2019). Listeria monocytogenes colonization in a newly established dairy processing facility. Int. J. Food Microbiol. *289*, 64–71. https://doi.org/10.1016/j.ijfoodmicro.2018.09.003.

Moreira, J.M.R., Teodósio, J.S., Silva, F.C., Simões, M., Melo, L.F., and Mergulhão, F.J. (2013). Influence of flow rate variation on the development of Escherichia coli biofilms. Bioproc.Biosyst. Eng. *36*, 1787–1796. https://doi.org/10.1007/s00449-013-0954-y.

Muhammad, M.H., Idris, A.L., Fan, X., Guo, Y., Yu, Y., Jin, X., Qiu, J., Guan, X., and Huang, T. (2020). Beyond risk: bacterial biofilms and their regulating approaches. Front. Microbiol. *11*, 928. https://doi.org/10.3389/fmicb.2020.00928.

Pang, X., Wong, C., Chung, H.-J., and Yuk, H.-G. (2019). Biofilm formation of Listeria monocytogenes and its resistance to quaternary ammonium compounds in a simulated salmon processing environment. Food Control *98*, 200–208. https://doi.org/10.1016/j.foodcont.2018.11.029.

Pereira, M.O., Kuehn, M., Wuertz, S., Neu, T., and Melo, L.F. (2002). Effect of flow regime on the architecture of a Pseudomonas fluorescens biofilm. Biotechnol.Bioeng. *78*, 164–171. https://doi.org/10.1002/bit.10189.

Purevdorj, B., Costerton, J.W., and Stoodley, P. (2002). Influence of hydrodynamics and cell signaling on the structure and behavior of Pseudomonas aeruginosa biofilms. Appl. Environ. Microbiol. *68*, 4457–4464. https://doi.org/10.1128/AEM.68.9.4457-4464.2002.

Rajab, F.H., Liauw, C.M., Benson, P.S., Li, L., and Whitehead, K.A. (2018). Picosecond laser treatment production of hierarchical structured stainless steel to reduce bacterial fouling. Food Bioprod.Process. *109*, 29–40. https://doi.org/10.1016/j.fbp.2018.02.009.

Recupido, F., Toscano, G., Tate, R., Petala, M., Caserta, S., Karapantsios, T.D., and Guido, S. (2020). The role of flow in bacterial biofilm morphology and wetting properties. Colloids Surf. B Biointerfaces *192*, 111047. https://doi.org/10.1016/j.colsurfb.2020.111047.

Simões, M., Simões, L.C., Machado, I., Pereira, M.O., and Vieira, M.J. (2006). Control of flow-generated biofilms with surfactants. Food Bioprod.Process. *84*, 338–345. https://doi.org/10.1205/fbp06022.

Simões, M., Simões, L.C., and Vieira, M.J. (2010). A review of current and emergent biofilm control strategies. LWT Food Sci. Technol. *43*, 573–583. https://doi.org/10.1016/j.lwt.2009.12.008.

Srey, S., Jahid, I.K., and Ha, S.-D. (2013). Biofilm formation in food industries: a food safety concern. Food Control *31*, 572–585. https://doi.org/10.1016/j.foodcont.2012.12.001.

Stoodley, P., Dodds, I., Boyle, J.D., and Lappin-Scott, H.M. (1999a). Influence of hydrodynamics and nutrients on biofilm structure. J.Appl.Microbiol.Symp.Suppl. *85*, 19S–28S.

Stoodley, P., Lewandowski, Z., Boyle, J.D., and Lappin-Scott, H.M. (1999b). The formation of migratory ripples in a mixed species bacterial biofilm growing in turbulent flow. Environ. Microbiol. *1*, 447–455.

Tide, C., Harkin, S.R., Geesey, G.G., Bremer, P.J., and Scholz, W. (1999). Influence of welding procedures on bacterial colonization of stainless steel weldments. J. Food Eng. *42*, 85–96. https://doi.org/10.1016/S0260-8774(99)00109-0.

Torotwa, I., and Ji, C. (2018). A study of the mixing performance of different impeller designs in stirred vessels using computational fluid dynamics. Designs *2*, 1–16. https://doi.org/10.3390/designs2010010.

Vieira, M.J., Melo, L.F., and Pinheiro, M.M. (1993). Biofilm formation: hydrodynamic effects on internal diffusion and structure. Biofouling *7*, 67–80.

Whitehead, K.A., Olivier, S., Benson, P.S., Arneborg, N., Verran, J., and Kelly, P. (2015). The effect of surface properties of polycrystalline, single phase metal coatings on bacterial retention. Int. J. Food Microbiol. *197*, 92–97. https://doi.org/10.1016/j.ijfoodmicro.2014.12.030.

iScience, Volume *24*

Supplemental information

Influence of the design of fresh-cut food washing tanks on the growth kinetics of *Pseudomonas fluorescens* biofilms

Laurent Bouvier, Charles Cunault, Christine Faille, Heni Dallagi, Laurent Wauquier, and Thierry Bénézech

Supplemental figures and legends

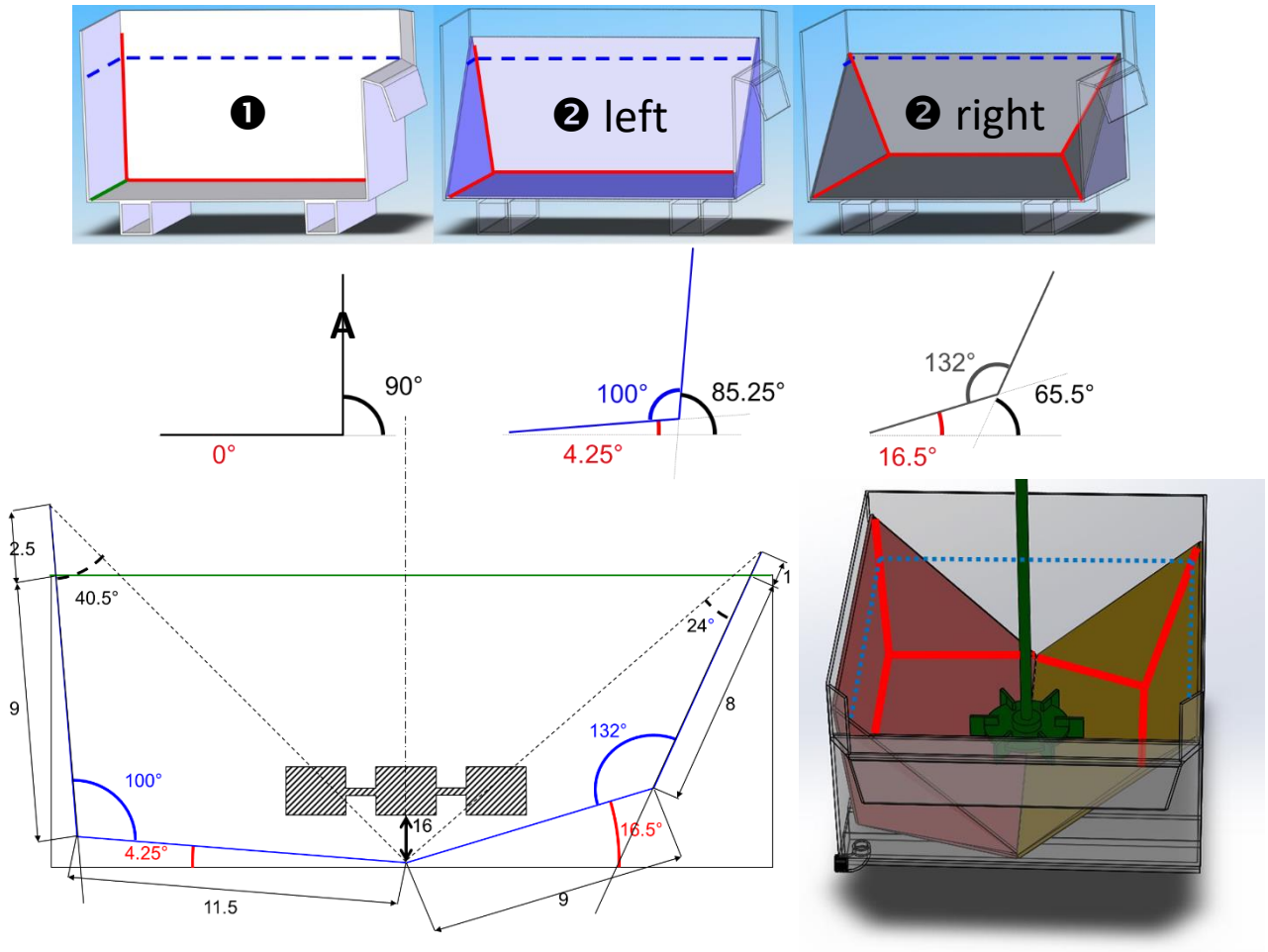


Figure S1: Vat geometry description in terms of angles and size (expressed in 10^{-2}m), Related to Figure 1. Vat 1 has right angles, horizontal and vertical surfaces; Vat 2 comprises two different parts with various vat wall inclinations, the impeller being at the middle of the tank.

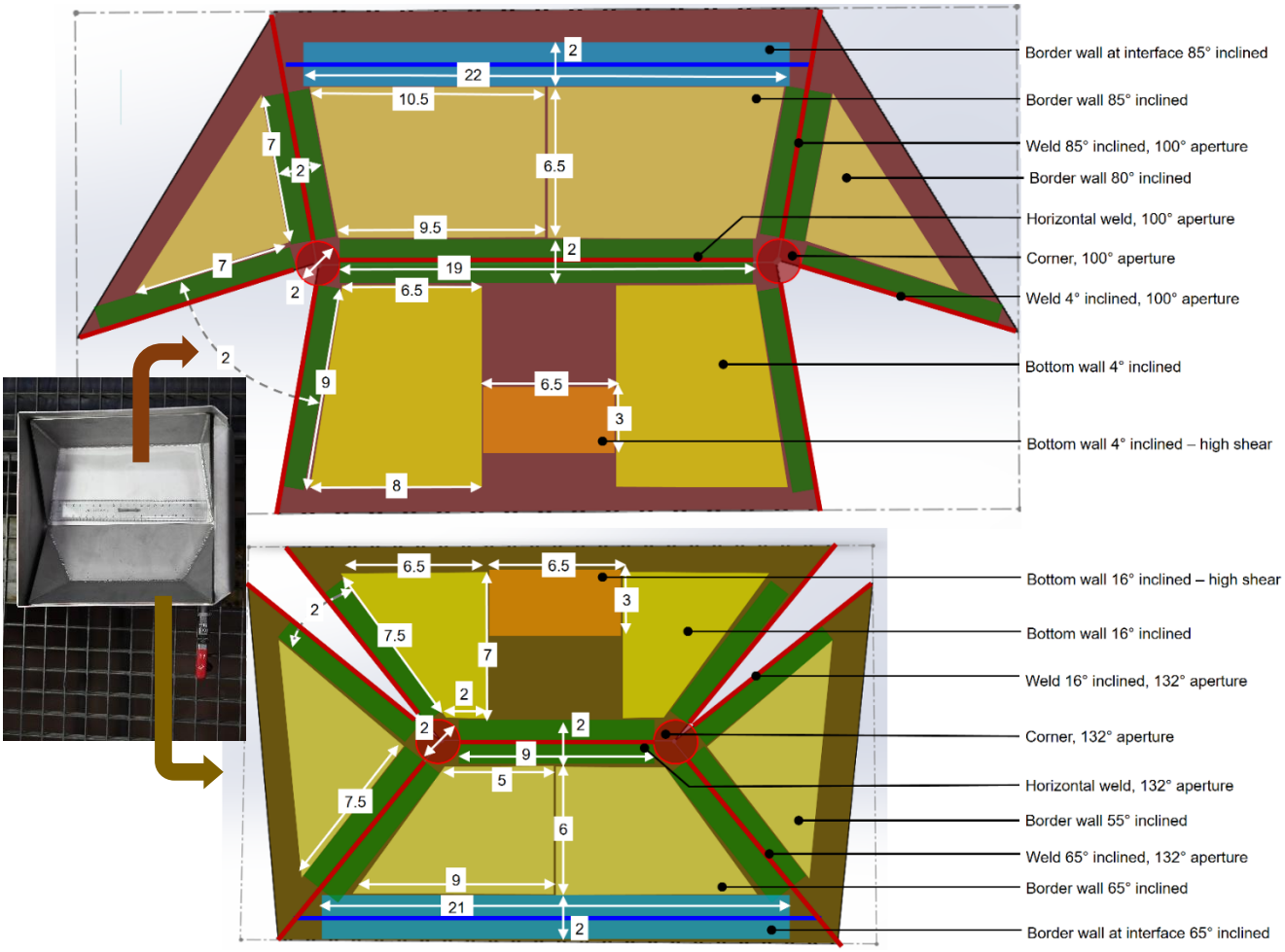


Figure S2: Swabbing areas in the alternative geometry vats (distances are expressed in 10^{-2} m), Related to Figures 3 and 4. A photo of the vat was displayed on the left with a ruler inside of 20 cm.

Transparent methods

Pilot rig

Experiments were performed on a pilot rig composed of a loop of a series of 8 stainless steel tanks (304L, 2B finish, average roughness (Ra) of 0.33 ± 0.05 µm), as previously described (Cunault et al., 2015). Briefly, each tank was filled with the contaminated suspension coming from the preceding tank and feeding the next tank by overflow. Apart from the first and the last tank, each tank was agitated using a Rushton impeller (Figure 1) at 300 rpm for the "traditional" shape (right angles, horizontal surfaces) or 215 rpm for the modified shape (no right angles, no horizontal surfaces). These speeds ensure an equivalent power dissipated per volume unit for the two configurations. The alternative

geometry versions are described in Figure S1. They meet general EHEDG hygienic design principles (EHEDG Document number 8, 2018 third edition) as all internal angles of 135° or less had a minimum radius of 3 mm and no sharp corners (≤ 90°). Two apertures were tested, 132° and 100° with no horizontal surfaces, the minimum angle with the horizontal being over 4°. The flow loop was filled with 73.5 L of soiling suspension maintained at 10°C and was set at a flow rate of 150 $L.h^{-1}$.

Biofilm formation

Pseudomonas fluorescens (PF1 strain) was isolated by the French Agency for Food, Environmental and Occupational Health & Safety (ANSES) from cleaning-in-place effluent. This strain was selected for the ability to grow in diluted nutrient media and form biofilms at 10◦C, a temperature close to that used in fresh-cut processing conditions (Charles Cunault et al., 2015). The initial (t_0) concentration of the soiling suspension was 10^6 $CFU.mL^{-1}$, obtained form an overnight culture of PF1 in TSB (Tryptone Soy Broth, Biokar, Beauvais, France at 30 °C agitated at 150 rpm. Biofilm formation kinetics were then carried out at 10 °C in standard nutrient TSB diluted ten times) in the pilot rig. The bacteria load on the test surfaces was assessed at the following times 0.75 (or 1), 6, 24, 30, 48 and 54 or 72 h. Trials were performed at least in triplicate. The protocol for surface contamination recovery has been previously detailed (Cunault et al., 2019). Briefly, each chosen surface area was swabbed with two cotton swabs (Copan, Brescia, Italy) previously soaked in peptone water without indole, diluted ten times with 0.5% TWEEN 80 (Sigma-Aldrich, France). The different zones of the vats analysed for biofilm formation are shown in Figure S2. On the flat areas, accurate swabbing was ensured by using a plastic template. The swabs were then vortexed for 30 s in peptone water to suspend the bacteria from the biofilm removed. The relevant dilutions were plated, and Petri dishes were then incubated for 48 h at 30 °C, prior to a CFU count. The plate-count provided an estimation of the Surface Microbial Load (SML) expressed in $Log_{10}(CFU.cm^{-2})$.

Growth curve fitting

Data obtained from bacterial counts, were fitted using the the Baranyi model as presented previously (Cunault et al., 2018). The Baranyi model was applied using the Excel add-in fitting curves DMfit v2.1 (http://www.combase.cc), based on Baranyi and Roberts (Baranyi and Roberts, 1994). This model used the four biological parameters N_0, N_{max}, λ and μmax which are, respectively, the initial load and the asymptotic maximal load, μ_{max} the maximal Napierian growth rate (h^{-1}) and λ the lag time (h).

As defined by Cunault et al. (Cunault et al., 2018), the biological signification of these parameters in terms of biofilm specificity are as follows. The initial Surface Microbial Load (SML) was null by definition in case of cleaned and sterile surfaces. Consequently, the estimated N_0 for the biofilm was based on the early adhesion phenomenon observed and quantified at 0.75 h (*i.e.* after the initial biofilm

installation step). The maximum Napierian growth rate μ_{max} identified for the biofilm growth, included a combination of phenomena, such as adhesion of new cells (cell recruitment), cell division, cell death and/or the cell detachment (Lewandowski et al., 1993). The lag time λ could not be explained by the sole adaptation of the bacteria to the growth conditions, insofar as the planktonic form had no lag time in our experiment. Thus, in the range of this study, Lag time was shown to be correlated to flow conditions and reflects the adhesion ability of the bacteria. The assessment of the fitting quality was carried out according to (Cunault et al., 2018).

CFD

A finite volume CFD simulation of the alternative geometry tank was achieved under OpenFOAM 6 software (© OpenCFD Ltd 2019, ESI Group). The non-modified geometry tank simulation results were described in Cunault et al. (2015).

The mesh was generated with a snappy hex mesh algorithm that guarantees a minimum mesh quality. It contains 696 590 cells, which gives sufficient precision and reasonable computational time. A dynamic mesh using an arbitrary mesh interface (AMI) algorithm functionality, was used for the rotating zone including the impeller (Rushton turbine). The rotating speed N was fixed at 215 rpm. The time discretization step started at 100 µs and then was automatically adjusted.

The Reynolds number ($\frac{\rho N D^2}{\mu}$) value is 25 000 indicating a turbulent flow regime, so the turbulence model k-Ω SST was activated in OpenFOAM.

The post-treatments were done under ParaView 5.8.1 software (Ahrens et al., 2005).

The wall shear stress ($WSS = \mu_{effective} \frac{\partial U}{\partial y}$) magnitude at the tank walls was computed over a period covering the last 0.3 s of simulation. For each defined zone (see swabbing areas in Figure 2), the average wall shear stresses at each time (every 0.01 s) was calculated. The minimum (WSSavmin) and the maximum (WSSavmax) were then calculated over a complete rotation of the impeller (0.3 s).

Statistical analyses

Trials were carried out at least in triplicate. Data obtained were compared to previous data (obtained on vats with horizontal and vertical walls for similar conditions (Cunault et al., 2018, 2015).Data were analysed by using SAS V9.4 software (SAS Institute, Gary, NC, USA). The Kruskal-Wallis Rank Sums tests were carried out to test if not the response variables corresponding to the growth parameters were normally distributed. In not normally distributed the Kruskal-Wallis Rank Sums tests were followed by a Pairwise Two-Sided Multiple Comparison Analysis (Dwass, Steel, Critchlow-Fligner Method). In case of the response variable is normally distributed, Analyses of Variance (ANOVA) were performed followed by multiple comparison procedures using Tukey's grouping (Alpha level = 0.05). Both analyses were performed to determine the impact of the geometry (corners, inclination, and aperture angle),

welds, proximity to the impeller when under the impeller (high WSS) or not (low WSS), interface areas air/water/wall and the trial on the biofilm growth parameters, either on the minimum or on the maximum of the average WSS for all swabbed areas over a complete impeller rotation.

Baranyi, J., Roberts, T.A., 1994. A dynamic approach to predicting bacterial growth in food. International journal of food microbiology 23, 277–294.

Cunault, C., Faille, C., Bouvier, L., Föste, H., Augustin, W., Scholl, S., Debreyne, P., Benezech, T., 2015. A novel set-up and a CFD approach to study the biofilm dynamics as a function of local flow conditions encountered in fresh-cut food processing equipments. Food and Bioproducts Processing 93, 217–223. https://doi.org/10.1016/j.fbp.2014.07.005

Cunault, C., Faille, C., Briandet, R., Postollec, F., Desriac, N., Benezech, T., 2018. Pseudomonas sp. biofilm development on fresh-cut food equipment surfaces – a growth curve – fitting approach to building a comprehensive tool for studying surface contamination dynamics. Food and Bioproducts Processing 107, 70–87. https://doi.org/10.1016/j.fbp.2017.11.001

Cunault, C., Faille, C., Calabozo-Delgado, A., Benezech, T., 2019. Structure and resistance to mechanical stress and enzymatic cleaning of Pseudomonas fluorescens biofilms formed in fresh-cut ready to eat washing tanks. Journal of Food Engineering 262, 154–161. https://doi.org/10.1016/j.jfoodeng.2019.06.006

Lewandowski, Z., Altobelli, S.A., Fukushima, E., 1993. NMR and microelectrode studies of hydrodynamics and kinetics in biofilms. Biotechnology progress 9, 40–45.